

POSITION-INVARIANT SURFACE RECOGNITION AND LOCALIZATION WITH SIMPLE INFRARED SENSORS FOR ROBOTICS APPLICATIONS

Tayfun Aytac and Billur Barshan

*Department of Electrical Engineering
Bilkent University, Bilkent, TR-06800 Ankara, Turkey
e-mail: {taytac, billur}@ee.bilkent.edu.tr*

Abstract

In this study, low-cost infrared sensors are used for the recognition of surfaces with different properties in a location-invariant manner. The intensity readings obtained with such sensors are highly dependent on the location and properties of the surface in a way which cannot be represented in a simple manner, complicating the recognition and localization process. We propose the use of angular intensity scans and present an algorithm to process them. This approach can differentiate different surfaces independent of their positions. Once the surface is identified, its position can also be estimated. The method is verified experimentally with the surfaces aluminum, white painted wall, brown craft paper, and styrofoam packaging material. A correct differentiate rate of 87% is achieved and the surfaces are localized within absolute range and azimuth errors of 1.2 cm and 1.0° , respectively. The method demonstrated shows that simple infrared sensors, when coupled with appropriate processing, can be used in mobile robot applications for differentiation and localization beyond their common usage as simple proximity sensors for object detection and collision avoidance.

Keywords: pattern recognition and feature extraction, surface recognition, position estimation, infrared sensors

1. Introduction

In this work, we consider the use of a simple infrared sensing system consisting of one emitter and one detector, for the purpose of surface recognition and localization. This paper complements our earlier work where we considered the differentiation and localization of objects with different geometries such as plane, corner, edge, and cylinder [1, 2]. Both tasks are of considerable interest for intelligent systems where there is need to distinguish objects for autonomous operation.

Infrared sensors are inexpensive, practical and widely available. The emitted light is reflected from the

surface and its intensity is measured at the detector. However, it is often not possible to make reliable distance estimates based on the value of a single intensity return because the return depends on both the surface and other properties of the reflecting object. Likewise, the properties of the surface cannot be deduced from simple intensity returns without knowing its distance and angular location. In this paper, we propose a scanning technique and algorithm that can differentiate surfaces in a manner which is invariant to their location. Once the surface properties are determined, its position (r, θ) can also be estimated.

The method we propose is scalable in the sense that the accuracy can be increased by increasing the number of reference scans without increasing the computational complexity of the differentiation and localization process. Position-invariant recognition and position estimation achieved in this paper differs from conventional pattern recognition techniques performed on conventional images in that here we work not on direct “photographic” images obtained by some kind of imaging system, but rather on angular intensity scans obtained by rotating a point sensor. What we differentiate are not patterns in a two-dimensional image whose coordinates we try to determine, but rather different kinds of surfaces, whose position with respect to the sensing system we need to estimate.

Typical use of infrared sensors in robotics applications include floor sensing, navigational referencing, and collision avoidance at short ranges [3]. They are used in door detection and mapping of openings in walls [4], as well as monitoring doors/windows of buildings and vehicles, and as “light curtains” for protecting an area. In [5], the properties of a planar surface at a known distance have been determined using the Phong illumination model, and using this information, the infrared sensor employed has been modeled as an accurate range finder for surfaces at short ranges. In [6], a number of commercially available light-based sensors are evaluated for robotic applications in outer space. In

[7], system and implementation issues in infrared proximity sensing in robot manipulator motion planning are discussed. Following this work, [8] describes a teleoperated whole-sensitive robot arm manipulator whose whole body is covered with a sensitive infrared skin sensor to detect nearby objects. Infrared sensors are used in door detection processes in [9]. However, to the best of our knowledge, no attempt has been made to simultaneously differentiate and estimate the position of several kinds of surfaces using a small number of simple, low-cost, point sensors.

2. Surface Recognition and Localization

The infrared sensor [10] used in this study consists of an emitter and detector, and provides analog output voltage proportional to the measured intensity. The detector window is covered with an infrared filter to minimize the effect of ambient light on the measurements. Indeed, when the emitter is turned off, the detector reading is essentially zero. The sensitivity of the device can be adjusted with a potentiometer to set the operating range of the system.

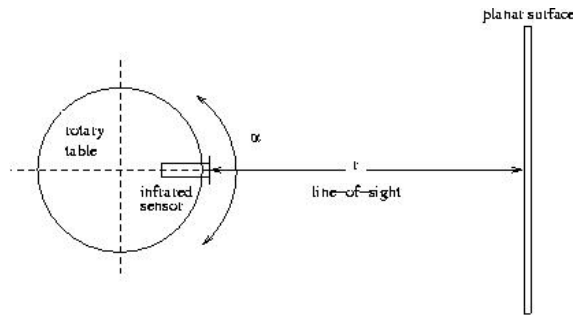


Figure 1: Top view of the experimental setup. Both the scan angle α and the surface azimuth θ are measured counter-clockwise from the horizontal axis.

The surfaces employed in this study are aluminum, white painted wall, brown craft paper, and styrofoam packaging material. Our method is based on angularly scanning the surfaces over a certain angular range. The infrared sensor is mounted on a 12 inch rotary table [11] (Fig. 1) to obtain angular scans $I(\alpha)$ from the surfaces. Reference data sets are collected for each surface type with 2.5 cm distance increments, ranging from 12.5 cm to 57.5 cm, at $\theta=0^\circ$. The resulting reference scans for the four surfaces are shown in Figs. 2-5. The intensity scans are θ -invariant but not r -invariant; changes in r do not result in any simple scaling. As we will see, these scans contain sufficient information to identify and localize different surfaces with a good degree of accuracy. Notice that the return signal intensities saturate at an intensity corresponding to about 11 V output voltage.

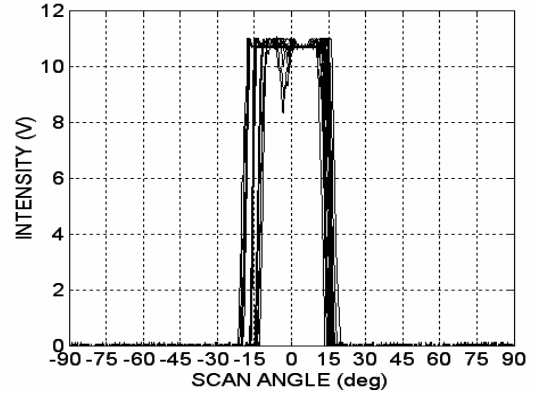


Figure 2: Intensity scans for aluminum at different distances.

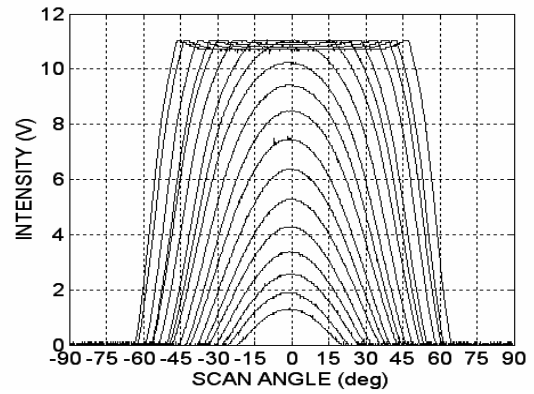


Figure 3: Intensity scans for white painted wall at different distances.

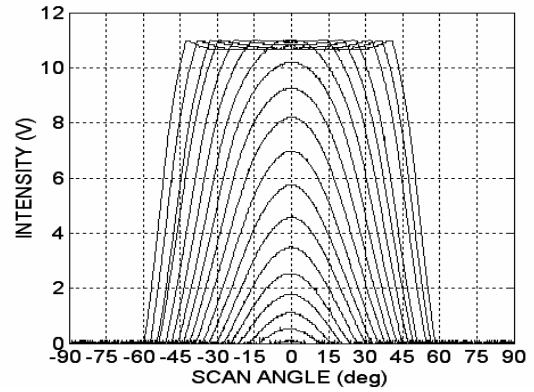


Figure 4: Intensity scans for brown craft paper at different distances.

We now describe how to recognize and determine the position of an arbitrarily located surface whose intensity scan has been observed. First, we check whether the observed scan $I(\alpha)$ exhibits saturation or not. This situation is treated separately as explained later in Section 2.3.

We start by identifying the surface. Unfortunately, direct comparison with the corresponding curves in Figs. 2-5 is not possible since we do not yet know the

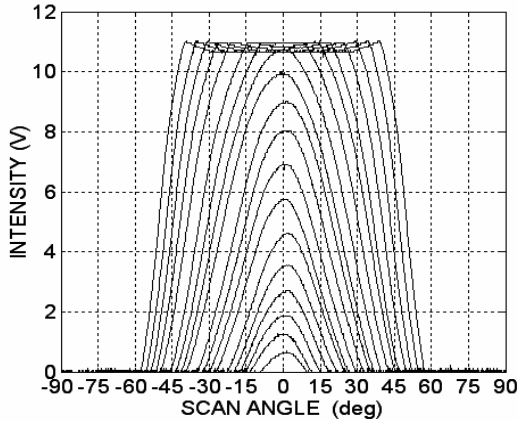


Figure 5: Intensity scans for styrofoam packaging material at different distances.

distance to the surface, and comparing with all the curves at all distances would be computationally very expensive. Therefore, we exploit the fact that the successive curves in Figs. 2-5 exhibit a monotonic dependence on distance. Furthermore, when an observed scan is compared to the several successive curves in any of Figs. 2-5, the two measures of difference between them described in Sections 2.1 and 2.2 below also exhibit a monotonic fall and rise around a single minimum. Therefore, we are assured that we will not be settling at a suboptimal point if we compare the observed scan not with all scans at all distances but only with the four scans (one for each surface type) whose central intensities are closest to that of the observed scan. Therefore, for unsaturated scans, only four comparisons need to be made. This remains the case even if the 2.5 cm increments are reduced to smaller values. This has the advantage that the accuracy of the system can be increased without increasing the cost of computation (although a greater number of scans do have to be stored). As a test, we also ran a version of the method where *eight* comparisons were made using the scans with the nearest central intensities both above *and* below the observed central intensity, and also using *all* of the scans shown in Figs. 2-5. These computationally more expensive approaches, exceedingly more so in the latter case, did not improve the results with respect to comparison with only four scans. In fact, since the systematic elimination of a priori suboptimal scans eliminates the small possibility that they will mistakenly be chosen as the best matching scan due to noise and other errors, results obtained by using all scans are found to be inferior to those obtained by using four scans.

Two alternative approaches, discussed below, are employed in performing the four comparisons.

2.1 Least-Squares Approach

First, we estimate the angular position θ of the surface as follows: Assuming the observed scan pattern is not saturated, we find the angular location of its maximum and the corresponding intensity value. This angular value, denoted θ_{MAX} , can be directly taken as an estimate of the angular position of the plane. Alternatively, the angular position can be estimated by finding the center-of-gravity (COG) of the scan as follows:

$$\theta_{COG} = \frac{\sum_{i=1}^n \alpha_i I(\alpha_i)}{\sum_{i=1}^n I(\alpha_i)} \quad (1)$$

where n is the number of samples in the angular scan. Ideally, these estimates would be equal, but in practice they differ by a small amount. We will consider the use of both alternatives when tabulating our results. From now on, we will refer to either estimate as the “center angle” of the scan.

Plots of the intensity at the center angle of each scan in Figs. 2-5 as a function of the distance at which that scan was obtained, play an important role in our method. Fig. 6 shows these plots for the maximum intensity case.

In this approach, we compare the intensity scan of the observed surface with the four reference scans by computing their least-squares differences after aligning their centers with each other. The mean-square difference between the observed scan and the four reference scans, one for each possible surface, is computed as follows:

$$\varepsilon_j = \sum_{i=1}^n [I(\alpha_i - \alpha_{align}) - I_j(\alpha_i)]^2 \quad (2)$$

where I_j , $j = 1, 2, 3, 4$ denote the four reference scans. Here, α_{align} is the angular shift which is necessary to align both patterns. The reference scan resulting in the smallest value of ε is declared as the observed surface. Once the type of the surface is determined, the range can be estimated by using linear interpolation on Fig. 6. Note that, this way, the accuracy of the method is not limited by the 2.5 cm spacing used in collecting the reference scans.

2.2 Matched Filtering Approach

As an alternative, we have also considered the use of matched filtering [12] to compare the observed and reference scans. The output of the matched filter is

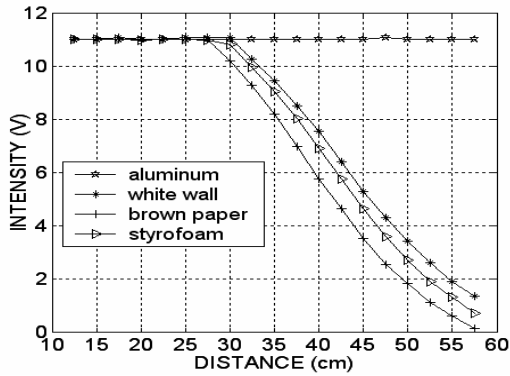


Figure 6: Central intensity versus distance curves for the different surfaces.

the cross-correlation between the observed intensity pattern and the j th reference scan normalized by the square root of its total energy:

$$y_j(l) = \frac{\sum_k I(\alpha_k) I_j(\alpha_{k-l})}{\sqrt{\sum_k [I_j(\alpha_k)]^2}} \quad (3)$$

The surface corresponding to the maximum cross-correlation peak is declared as the observed surface type, and the angular position of the correlation peak directly provides an estimate of the azimuth angle of the surface. Then, the distance is estimated by using linear interpolation on Fig. 6 with the intensity value at the azimuth estimate.

2.3 Saturated Scans

If saturation is detected in the observed scan, special treatment is necessary. In the least-squares approach, the mean-square difference between the aligned observed scan and *all* the saturated reference scans are computed and the reference scan with the minimum mean-square difference is chosen. The range estimate of the surface is taken as the distance corresponding to the scan resulting in the minimum mean-square difference. Similarly, for the matched filter, correlation between the observed scan and *all* the stored saturated reference scans is computed and the reference scan resulting in the highest correlation peak is selected. The range estimate is again taken as that of the best matching scan.

It should be noted that, in the saturated case, range estimation accuracy is limited by the 2.5 cm interval at which the reference scans were taken. If this accuracy is not satisfactory, it can be improved by reducing the 2.5 cm intervals. We underline that the 2.5 cm interval does not limit the range estimation accuracy in the unsaturated case, where accurate interpolation is possible from Fig. 6.

In the unsaturated case, the azimuth could be estimated by taking the angular value corresponding to either the maximum value of the intensity curve or its COG. In the case of saturated scans, a single maximum may not be observed but the COG can still be used to reliably estimate the azimuth. Even when the maximum intensity is used for the unsaturated scans, the COG approach is used for the saturated scans.

3. Experimental Verification and Discussion

In this section, we experimentally verify the proposed method by locating the surfaces at randomly selected distances r and azimuth angles θ and collecting a total of 100 test scans. The surfaces are randomly located at ranges from 12.5 cm up to 57.5 cm and azimuths from -45° to 45° .

The results of least-squares based surface differentiation are displayed in Tables 1 and 2 in the form of surface confusion matrices. Table 1 gives the results obtained using the maximum intensity values, and Table 2 gives those obtained using the intensity value at the COG of the scans. The average correct classification rates obtained by using the maximum intensity and the COG variations of the least-squares approach are 81% and 82%, respectively.

Matched filter differentiation results are presented in Table 3. The average accuracy of differentiation over all surfaces is 87%, which is better than that obtained with the least-squares approach. In [1], where we dealt with the differentiation of targets with different geometries as opposed to different surfaces treated here, the least-squares approach resulted in a differentiation accuracy of 93% and 89% and the matched filtering approach resulted in an accuracy of 97%. Based on these results, we conclude that differentiating targets with different surfaces is considerably more difficult than differentiating targets with different geometries.

As shown in the tables, aluminum is always correctly identified regardless of which method is used, due to its distinctive signature. The remaining surfaces are comparable in terms of their correct identification percentages. Brown craft paper is the surface most confused with others, especially styrofoam. Although the intensity scans of these two surfaces do not resemble each other in the unsaturated region, their saturated scans are similar, contributing to the misclassification rate. Nearly all misclassified surfaces are located at nearby ranges where the return signal intensities are saturated. This means that the misclassification rate can be reduced by increasing the lower limit of the range interval at the cost of reducing the operating range.

Table 1: Surface confusion matrix: least-squares based recognition (maximum intensity variation). (AL: aluminum, WW: white wall, BP: brown paper, ST: styrofoam).

surface	recognition result				total
	AL	WW	BP	ST	
AL	25	-	-	-	25
WW	-	20	3	2	25
BP	-	5	17	3	25
ST	-	-	6	19	25
total	25	25	26	24	100

Table 2: Surface confusion matrix: least-squares based recognition (COG variation).

surface	recognition result				total
	AL	WW	BP	ST	
AL	25	-	-	-	25
WW	-	20	3	2	25
BP	-	4	18	3	25
ST	-	-	6	19	25
total	25	24	27	24	100

Table 3: Surface confusion matrix: matched filter based recognition.

surface	recognition result				total
	AL	WW	BP	ST	
AL	25	-	-	-	25
WW	-	21	3	1	25
BP	-	1	21	3	25
ST	-	-	5	20	25
total	25	22	29	24	100

Table 4: Absolute range and azimuth estimation errors over all surfaces.

method		AL	WW	BP	ST	ave. err.
		least-squares (max)	r (cm)	2.4	1.3	1.3
	θ (deg)	0.8	1.9	1.6	0.8	1.3
least-squares (COG)	r (cm)	2.4	1.3	1.3	0.9	1.5
	θ (deg)	0.8	1.0	1.6	0.8	1.1
matched filter	r (cm)	1.7	1.2	1.0	0.8	1.2
	θ (deg)	0.8	1.1	1.6	0.7	1.0

The average absolute range and azimuth estimation errors for the different approaches are presented in Table 4 over all surface types. As seen in the table, using the maximum intensity and COG variations of the least-squares approach, the surface ranges are estimated with average absolute range error of 1.5 cm in both cases. Matched filtering results in an average absolute range error of 1.2 cm which is better than that obtained with the least-squares approach. The greatest contribution to the range errors comes from surfaces which are incorrectly recognized. If we average over only correctly recognized surfaces, the average absolute range errors become 1.0 cm, 1.1 cm, and 1.2 cm for the maximum intensity and COG

variations of least-squares and the matched filter approaches, respectively. Since these three numbers are relatively closer than the corresponding numbers in Table 4, we may conclude that the superior range accuracy of matched filtering is mostly a consequence of its superior differentiation accuracy.

The major contribution to range errors comes from saturated scans where linear interpolation from Fig. 6 cannot be employed to obtain better range estimates. Consequently, surfaces for which saturation occurs over a greater portion of the operating range exhibit greater range estimation errors, with aluminum being the worst.

As for azimuth estimation, matched filtering results in an average absolute estimation error of 1.0° , which is the best among the approaches compared. Averaging the azimuth errors over only correctly differentiated surfaces does not result in significant changes. This is due to the fact that azimuth estimation is not dependent on correct differentiation. The COG variation is, on the average, better than the maximum intensity variation in azimuth estimation due to the fact that COG based calculations average out the noise in the return signal intensities.

We have also considered expanding the range of operation of the system. As an example, changing the operating range from [12.5 cm, 57.5 cm] to [5 cm, 60 cm], results in a reduction of the correct differentiation percentage from 87% to 80%. This reduction in performance is mostly a consequence of highly saturated scans and scans with very low intensities, both of which are prone to greater errors.

Light reflected from a surface consists of specular and diffuse components. The specular component is concentrated where the reflection angle equals the incidence angle, whereas the diffuse component is spread in all directions with a cosine factor. For different types of surfaces, the contribution of these two components and the rate of decrease of intensity with the scan angle α is different. It is this difference which results in a characteristic intensity scan pattern (signature) for each surface, enabling us to distinguish them without knowing their positions. In contrast, a system relying only on reflected energy could not distinguish between a highly reflecting distant object and a less reflecting nearby one. Occasionally, two very distinct surfaces may have intensity scans with very similar dependence on α , in which case they cannot be reliably differentiated with the present method.

4. Conclusions

In this study, differentiation and localization of four types of surfaces is achieved using an inexpensive

infrared emitter and detector pair. Different approaches are compared in terms of correct differentiation, and range and azimuth estimation accuracy. The method demonstrated shows that simple infrared sensors, when coupled with appropriate processing, can be used to extract a significantly greater amount of information than they are commonly employed for in robotics applications. A typical use of the demonstrated system would be in mobile robotics in surveying an unknown environment composed of several different types of surfaces, or industrial applications where different materials must be identified and separated.

The main accomplishment of this study is that even though the intensity patterns are highly dependent on surface location and properties, and this dependence cannot be represented by a simple relationship, we achieve position-invariant differentiation of different types of surfaces. A correct differentiation rate of 87% over all surface types is achieved and surfaces are localized within absolute range and azimuth errors of 1.2 cm and 1.0° , respectively. The method we propose is scalable in the sense that the accuracy can be increased by increasing the number of reference scans without increasing the computational cost.

In earlier work, we had considered differentiation and localization of objects having different geometries such as plane, corner, edge, and cylinder [1, 2], as opposed to the differentiation and localization of different surfaces considered in this paper. 97% and 91.3% correct differentiation rates were achieved in [1] and [2], respectively. Comparing these with the 87% correct differentiation achieved in this paper, we conclude that specular/diffuse reflection characteristics are not as distinctive as geometric reflection characteristics.

Current work investigates the deduction of both the surface type and also the geometry of the target from its intensity scan without knowing its location. Preliminary results indicate that the method of the present paper can be applied to this case by treating the combination of a particular geometry and particular surface as a generalized target type. Also being considered is the parametric modeling and representation of intensity scans rather than the use of the intensity scan vectors themselves.

Acknowledgment

This research was supported by TÜBİTAK under BDP and 197E051 grants. The authors would like to thank the Robotics Research Group of the University of Oxford for donating the infrared sensors.

References

- [1] T. Aytaç and B. Barshan, "Differentiation and localization of targets using infrared sensors," **Opt. Commun.**, vol. 210, no. 1-2, pp. 25-35, September 2002.
- [2] T. Aytaç and B. Barshan, "Rule-based target differentiation and position estimation based on infrared intensity measurements," **Opt. Eng.**, vol. 42, no. 6, pp. 1766-1771, June 2003.
- [3] H. R. Everett, *Sensors for Mobile Robots, Theory and Application*. 289 Linden St., Wellesley, MA: A K Peters, Ltd., 1995.
- [4] A. M. Flynn, "Combining sonar and infrared sensors for mobile robot navigation," **Int. J. Robot. Res.**, vol. 7, no. 6, pp. 5-14, December 1988.
- [5] P. M. Novotny and N. J. Ferrier, "Using infrared sensors and the Phong illumination model to measure distances," in Proc. IEEE Int. Conf. Robot. Automat., pp. 1644-1649, Detroit, MI, 10-15 May 1999.
- [6] L. Korba, S. Elgazzar, and T. Welch, "Active infrared sensors for mobile robots," **IEEE Trans. Instrum. Meas.**, vol. 43, no. 2, pp. 283-287, April 1994.
- [7] E. Cheung and V. J. Lumelsky, "Proximity sensing in robot manipulator motion planning: system and implementation issues," **IEEE Trans. Robot. Automat.**, vol. 5, no. 6, pp. 740-751, December 1989.
- [8] V. J. Lumelsky and E. Cheung, "Real-time collision avoidance in teleoperated whole-sensitive robot arm manipulators," **IEEE Trans. Syst. Man Cybern.**, vol. 23, no. 1, pp. 194-203, January/February 1993.
- [9] G. Beccari, S. Caselli, and F. Zanichelli, "Qualitative spatial representations from task-oriented perception and exploratory behaviors," **Robot. Autom. Syst.**, vol. 25, no. 3/4, pp. 147-157, 30 November 1998.
- [10] Matrix Elektronik, AG, Kirchweg 24 CH-5422 Oberehrendingen, Switzerland, IRS-U-4A Proximity Switch Datasheet, 1995.
- [11] Arrick Robotics, P.O. Box 1574, Hurst, Texas, 76053, URL: www.robotics.com/rt12.html, RT-12 Rotary Positioning Table, 2002.
- [12] J. W. Goodman, *Introduction to Fourier Optics*, New York: McGraw-Hill, 2nd ed., 1996, pp. 246-249.